Progress In Electromagnetics Research, Vol. 126, 449–461, 2012

42.13 GBIT/S 16QAM-OFDM PHOTONICS-WIRELESS TRANSMISSION IN 75–110 GHz BAND

L. Deng[1,*], D. M. Liu[1], X. D. Pang[2], X. Zhang[2], V. Arlunno[2], Y. Zhao[2], A. Caballero[2], A. K. Dogadaev[2], X. B. Yu[2], I. T. Monroy[2], M. Beltrán[3], and R. Llorente[3]

[1]College of Optoelectronics Science and Engineering, Huazhong University of Science and Technology, Wuhan 430074, China

[2]DTU Fotonik, Department of Photonics Engineering, Technical University of Denmark, Kgs. Lyngby DK-2800, Denmark

[3]Valencia Nanophotonics Technology Center, Universidad Politcnica de Valencia, Valencia 46022, Spain

Abstract—We present a simple architecture for realizing high capacity W-band (75–110 GHz) photonics-wireless system. 42.13 Gbit/s 16QAM-OFDM optical baseband signal is obtained in a seamless 15 GHz spectral bandwidth by using an optical frequency comb generator, resulting in a spectral efficiency of 2.808 bits/s/Hz. Transparent photonic heterodyne up-conversion based on two free-running lasers is employed to synthesize the W-band wireless signal. In the experiment, we program an improved DSP receiver and successfully demonstrate photonics-wireless transmission of 8.9 Gbit/s, 26.7 Gbit/s and 42.13 Gbit/s 16QAM-OOFDM W-band signals, with achieved bit-error-rate (BER) performance below the forward error correction (FEC) limit.

1. INTRODUCTION

Due to the explosive bandwidth growth expected from the emerging wireless applications such as 3-D face-to-face communication and super Hi-Vision/Ultra High Definition TV data (more than 24 Gbit/s) [1], wireless communication links with very large capacity (towards 100 Gbit/s) are envisioned. However, current microwave wireless systems can provide only tens of Mbit/s because of regulatory constraints [2–4]. An alternative solution is to shift the carrier frequency

Received 30 January 2012, Accepted 22 March 2012, Scheduled 26 March 2012

* Corresponding author: Lei Deng (leide@fotonik.dtu.dk).

to the millimeter-wave bands, where several GHz unregulated available bandwidths are able to potentially provide very high capacity. Compared to 60 GHz [5, 6] and 120 GHz bands, the unregulated W-band (75–110 GHz) is recently attracting increasing research interests due to less air absorption loss and larger available frequency window [7, 8]. Furthermore, radio over fiber techniques in the W-band fiber-wireless system are expected to enable not only broadband services and wide wireless coverage, but also seamless integration of wireless links into future optical networks.

As a highly spectral efficient and flexible modulation technique, orthogonal frequency division multiplexing (OFDM) has been widely used in current wireless system [9, 10], since it is robust against fiber dispersion effects (chromatic dispersion and polarization mode dispersion) in optical fiber channels and wireless multipath fading in wireless channels. In the 60 GHz band, OFDM technique has already been used to realize 27 Gbit/s [11] and 28 Gbit/s [12] 16-quadrature amplitude modulation (QAM)-OFDM fiber-wireless links with coherent optical up-conversion at a modulator. In the W-band, quadrature phase-shift keying (QPSK) and 16-QAM have also been used to achieve 20 Gbit/s [13] and 40 Gbit/s [14] wireless links. So far, no high speed OFDM W-band wireless transmission system has been reported. In these reported 60 GHz band and W-band schemes, hybrid photonic-electronic up-conversion (coherent method) is used to generate the high wireless carrier frequency, and 2.5 m wireless transmission with achieved performance slightly above the forward error correction (FEC) limit in [11] and 30 mm wireless transmission with achieved performance below the FEC limit in [13, 14] are demonstrated. Recently, a photonic up/down-conversion (incoherent method) with RF/bit-rate transparency has also been proposed for a 40 Gbit/s OFDM W-band system without air transmission [15]. The wireless transmission demonstration of very high speed OFDM W-band signals will therefore contribute to the needed development of ultra-broadband wireless communication technology.

In this paper, we present for the first time, a high speed and scalable photonics-wireless transmission system in 75–110 GHz by combining the spectral efficient OFDM modulation and coherent optical frequency division multiplexing techniques. By using optical heterodyne mixing of a high-speed optical OFDM baseband signal with a free-running laser, the system can seamlessly generate a high capacity W-band wireless signal, while preserving transparency to bit rates, modulation format and RF carrier. A digital signal processing (DSP) based receiver benefits us with significant complexity reduction and increased flexibility. Furthermore, 0.6 m photonics-

wireless transmission of 42.13 Gbit/s OOFDM signal is successfully achieved in the experiment. We also demonstrate the capacity and bandwidth scalability of the proposed system.

2. PRINCIPLE OF HETERODYNE UP-CONVERSION AND DOWN-CONVERSION

The block diagram of the proposed system is shown in Fig. 1. In the transmitter, the optical in-phase/quadrature-modulated OFDM signal is heterodyne mixed with a free running laser to generate the W-band wireless signal. The baseband electrical OFDM signal $E_{\mathrm{OFDM}}(t)$, the optical OFDM signal $E_s(t)$ and the beating laser $E_c(t)$ can be represented as:

$$\begin{aligned} E_{\mathrm{OFDM}}(t) &= I(t) + jQ(t), \\ E_s(t) &= \sqrt{P_s} \cdot E_{\mathrm{OFDM}}(t) \cdot \exp[-j(\omega_s t + \phi_s(t))], \\ E_c(t) &= \sqrt{P_c} \cdot \exp[-j(\omega_c t + \phi_c(t))], \end{aligned} \tag{1}$$

where $I(t)$ and $Q(t)$ are the real and image part of the electrical baseband OFDM signal. P_s, ω_s and $\phi_s(t)$ represent the optical power, angular frequency and phase of the signal laser respectively, so as P_c, ω_c and $\phi_c(t)$ for the beating laser. The combined signal is beating at a photodiode for heterodyne up-conversion, and the output signal $E(t)$ could be described as:

$$\begin{aligned} E(t) \;\propto\; |E_s(t) + jE_c(t)|^2 &= P_s + P_c + E_{\mathrm{RF}}(t), \\ E_{\mathrm{RF}}(t) = 2\sqrt{P_s P_c} \cdot [I(t) \cdot \sin(\triangle\omega t + \triangle\phi(t)) &\\ +Q(t) \cdot \cos(\triangle\omega t + \triangle\phi(t))], &\\ \triangle\omega = \omega_c - \omega_s, \quad \triangle\phi(t) = \phi_c(t) - \phi_s(t), & \end{aligned} \tag{2}$$

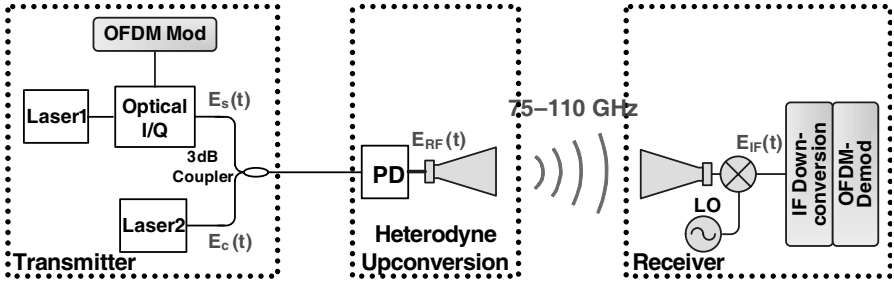

Figure 1. The block diagram of the proposed photonics-wireless system.

where $E_{\mathrm{RF}}(t)$ represents the generated W-band signal with carrier frequency of $\triangle\omega$, and the phase noise of signal laser and beating laser are included in $\triangle\phi(t)$. By using a horn antenna, the W-band wireless signal is detected after air transmission. A W-band balanced mixer and a sinusoidal LO signal are used for electrical down-conversion. The LO signal is expressed as $E_{\mathrm{LO}}(t) = \sqrt{P_{\mathrm{LO}}} \cdot \cos(\omega_{\mathrm{LO}}t + \phi_{\mathrm{LO}}(t))$, here P_{LO}, ω_{LO} and $\phi_{\mathrm{LO}}(t)$ represent the power, angular frequency and phase of the LO signal, respectively. After the electrical down-conversion, the generated intermediate frequency (IF) signal can be described as:

$$\begin{aligned} E_{\mathrm{IF}}(t) &= \langle E_{\mathrm{RF}}(t) \cdot E_{\mathrm{LO}}(t) \rangle \\ &= \sqrt{P_s P_c P_{\mathrm{LO}}} \cdot [I(t) \cdot \sin(\triangle\omega_{\mathrm{IF}}t + \triangle\phi_{\mathrm{IF}}(t)) \\ &\quad + Q(t) \cdot \cos(\triangle\omega_{\mathrm{IF}}t + \triangle\phi_{\mathrm{IF}}(t))], \\ \triangle\omega_{\mathrm{IF}} &= \omega_{\mathrm{LO}} - (\omega_c - \omega_s), \quad \triangle\phi_{\mathrm{IF}}(t) = \phi_{\mathrm{LO}}(t) - (\phi_c(t) - \phi_s(t)), \end{aligned} \tag{3}$$

where $\triangle\omega_{\mathrm{IF}}$ and $\triangle\phi_{\mathrm{IF}}(t)$ represent the angular frequency and phase of the IF carrier signal. The phase noise of the signal laser, beating laser and LO signal are all included in $\triangle\phi_{\mathrm{IF}}(t)$. After electrical down-conversion, 2-steps demodulation algorithms are performed in our DSP receiver. In the first step, IF frequency down-conversion is implemented by multiplying IF signal $E_{\mathrm{IF}}(t)$ by $\exp(-j\triangle\omega_{\mathrm{IF}}t)$, as expressed in Eq. (4). A low-pass filter is used to filter out the high-order items, and the generated signal $E_1(t)'$ is described in Eq. (4) as well.

$$\begin{aligned} E_1(t) &= E_{\mathrm{IF}}(t) \cdot \exp(-j\triangle\omega_{\mathrm{IF}}t), \\ E_1(t)' &= \frac{1}{2}\sqrt{P_s P_c P_{\mathrm{LO}}} \cdot [I(t) \cdot \sin(\triangle\phi_{\mathrm{IF}}(t)) - jI(t) \cdot \cos(\triangle\phi_{\mathrm{IF}}(t)) \\ &\quad + Q(t) \cdot \cos(\triangle\phi_{\mathrm{IF}}(t)) + jQ(t) \cdot \sin(\triangle\phi_{\mathrm{IF}}(t))] \\ &= -\frac{1}{2}j\sqrt{P_s P_c P_{\mathrm{LO}}} \cdot (I(t) + jQ(t)) \cdot \exp(j\triangle\phi_{\mathrm{IF}}(t)). \end{aligned} \tag{4}$$

As shown in Eq. (4), the $I(t) + jQ(t)$ item is the desired OFDM signal, and the $\exp(j\triangle\phi_{\mathrm{IF}}(t))$ item is the phase noise which need to be removed. Therefore, in the second step, frequency and channel estimation and pilot-based phase noise estimation algorithms are used for the OFDM demodulation in our experiment.

3. EXPERIMENTAL SETUP

Figure 2 shows the experimental setup of the proposed high capacity 16QAM-OFDM W-band wireless transmission system. At the 16QAM-OOFDM transmitter, an arbitrary waveform generator (AWG, Tektronix AWG 7122C) is performed to generate the OFDM

waveform. In the signal generator, a data stream with a pseudo-random bit sequence (PRBS) length of $2^{15} - 1$ is mapped onto 72 16-QAM subcarriers, which are converted into the time domain together with 8 pilot subcarriers, one unfilled DC subcarrier, and 47 unfilled edge subcarriers by applying 128-point inverse fast Fourier transform (IFFT) [16]. The cyclic prefix is 1/10 of the IFFT length resulting in an OFDM symbol size of 141. To facilitate time synchronization and channel estimation, 10 training symbols are inserted at the beginning of each OFDM frame that contains 150 data symbols. The real and imaginary parts of the OFDM signal are clipped and converted to analog signals by two D/A converters operating at 5 GS/s with a D/A resolution of 10 bits. The generated OFDM signals are filtered by two antialiasing low-pass filters (LPFs) with 2.5 GHz bandwidth, and then used to modulate a 100 kHz-linewidth continuous-wave (CW) external cavity laser (ECL, $\lambda_1 = 1552.886$ nm) at an optical in-phase/quadrature (I/Q) modulator biased at its null point. An optical OFDM signal at a net data rate of 9.57 Gbit/s ($5\,\text{GSa/s} \times 4 \times 72 \div 141 \times 150 \div 160$) with a bandwidth of 3.164 GHz ($5\,\text{GSa/s} \times 81 \div 128$) is formed. An erbium-doped fiber amplifier (EDFA) and an optical filter with 0.8 nm bandwidth are used to compensate the loss of optical I/Q modulator and filter out the outband noise, respectively.

Subsequently, the optical OFDM signal is launched into an optical frequency comb generator employing an overdriven Mach-Zehnder modulator (MZM). The MZM is biased in its nonlinear region by equalizing the power of the central 3 comb lines. The frequency spacing of the comb lines is set to 3.125 GHz, 4 GHz and 5 GHz for scalability testing. In the case of 4 GHz comb spectral spacing, 72 OFDM

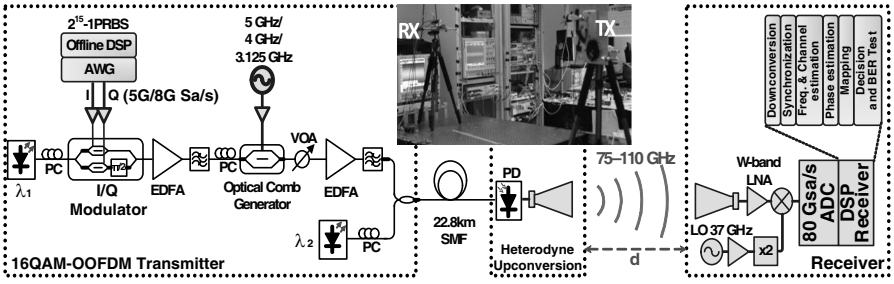

Figure 2. Experimental setup for the proposed 16QAM-OOFDM W-band transmission system. Inset photograph: Global view of the wireless link setup with wireless transmitter (TX) and receiver (RX). AWG: Arbitrary waveform generator. PC: Polarization controller. VOA: Variable optical attenuator.

subcarriers are adopted in each comb-line to obtain an optical OFDM signal at 28.72 Gbit/s (3lines $\times$ 5 GSa/s $\times$ 4 $\times$ 72 $\div$ 141 $\times$ 150 $\div$ 160) with a spectral bandwidth of 11.164 GHz (5 GSa/s $\times$ 81 $\div$ 128 + 2 $\times$ 4 GHz). In the case of 3.125 GHz spacing, one edge subcarrier of the OFDM signal in each comb-line is deleted to avoid the inter-symbol interference (ISI), resulting in an optical OFDM signal at 28.32 Gb/s with a spectral bandwidth of 9.375 GHz (3lines $\times$ 5 GSa/s $\times$ 80 $\div$ 128). In the case of 5 GHz spacing, the sampling rate of AWG is set to 8 GSa/s, and 71 OFDM subcarriers are adopted in each comb-line to obtain an optical OFDM signal at 45.31 Gbit/s (3lines $\times$ 8 GSa/s $\times$ 4 $\times$ 71 $\div$ 141 $\times$ 150 $\div$ 160) with a spectral bandwidth of 15 GHz (3lines $\times$ 8 GSa/s $\times$ 80 $\div$ 128). The generated optical signal at the output of optical comb generator is seamless in the case of 3.125 GHz and 5 GHz spectral spacing, because the comb spacing is integral multiple of the OFDM subcarrier spacing and all of the OFDM subcarriers from different comb lines are orthogonal to each other. The second EDFA and optical filter with 0.8 nm bandwidth are used to compensate the insertion loss of the optical comb generator and to eliminate the high-order modulation sidebands. It is noted that these 3-lines OFDM signals are correlated, and the de-correlation of 3-lines and the effect of inter-channel interference (ICI) between different lines are under further investigation from a practical point of view.

The optical 3-lines 16QAM-OFDM signal is then combined with a 100 kHz linewidth free-running CW laser (λ_2 = 1553.574 nm)

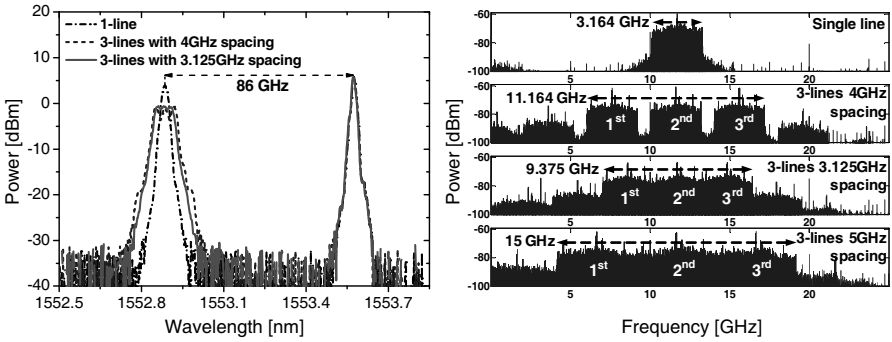

Figure 3. (a) The optical spectra of optical baseband signal (single-line, 3-lines with 3.125 GHz spacing and 4 GHz spacing) and local oscillator (LO). (b) Electrical spectra of 16QAM-OOFDM signal (single-line, 3-lines with 3.125 GHz, 4 GHz and 5 GHz spacing) after down-conversion mixer.

for optical transparent generation of W-band wireless signals. The measured optical spectra of single-line, 3-lines with 3.125 GHz and 4 GHz spacing at the input of the photodiode are shown in the Fig. 3(a). After 22.8 km of standard single mode fiber (SSMF) propagation, the combined optical signal is heterodyne mixed in a 100 GHz bandwidth photodiode (PD, u^2t XPDV4120R) at the remote antenna site to generate a W-band wireless signal, which is then fed to a W-band horn antenna with 24 dBi gain. A photograph of the global view of the wireless link is inserted in Fig. 2 as well. After air transmission, the signal is detected by a horn antenna with 25 dBi gain and amplified by a W-band 25 dB gain low-noise amplifier (LNA, Radiometer Physics W-LAN). A W-band balanced mixer driven by a 74 GHz sinusoidal LO signal after frequency doubling from a 37 GHz signal synthesizer (Rohde & Schwarz SMF 100A) is employed for electrical down-conversion. The electrical spectra of intermediate frequency (IF) signals after down-conversion for single-line, 3-lines with 3.125 GHz, 4 GHz and 5 GHz spacing are shown in Fig. 3(b).

An 80 GSa/s real-time sampling oscilloscope with 32 GHz analog bandwidth (Agilent DSAX93204A) is used to capture the IF signals. Offline signal demodulation is then performed by a DSP-based receiver consisting of frequency down-conversion, time synchronization, frequency and channel estimation, pilot-based phase estimation, data mapping and bit error rate (BER) tester. Furthermore, we program one-tap equalizer and an effective channel estimation algorithm by combining the intra symbol frequency-domain averaging (ISFA) [17, 18]

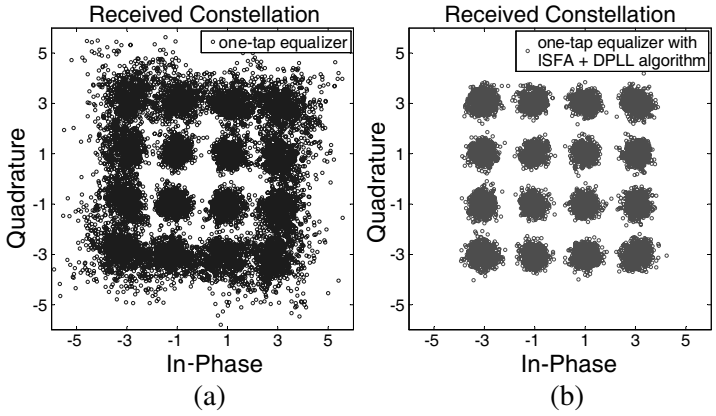

Figure 4. Received constellations of 9.57 Gbit/s (single-line) W-band signal after 22.8 km SMF and 0.65 m air distance transmission without ISFA-DPLL (BER of 1.49×10^{-2}) and with ISFA-DPLL (BER of 2.33×10^{-5}).

and digital phase-locked loop (DPLL) to mitigate the dispersion and nonlinearity (e.g., four-wave mixing) effects induced by fiber and wireless transmission. We can clearly observe the performance improvement by comparing the received constellations with/without ISFA-DPLL for 9.57 Gb/s (single-line) 16QAM-OFDM W-band signal after 22.8 km SMF and 0.65 m air transmission in Fig. 4.

4. EXPERIMENTAL RESULTS AND DISCUSSIONS

The millimeter-wave carrier frequency is set to 86 GHz in our experiment to match the central operation frequency of the electrical mixer. To test the system scalability, we measure the performance for single line, 3-lines with 3.125 GHz, 4 GHz and 5 GHz spacing at bit rates of 9.57 Gbit/s, 28.32 Gbit/s, 28.72 Gbit/s and 45.31 Gbit/s, respectively. After considering the 7% Reed-Solomon forward-error correction (FEC) overhead, the effective net bit rate is 8.9 Gbit/s, 26.33 Gbit/s, 26.7 Gbit/s, and 42.13 Gbit/s, respectively.

Figure 5(a) shows the measured BER in terms of the received optical power into the PD after different air transmission distances in optical back-to-back (B2B) for both single-line and 3-lines with 4 GHz spacing. In the case of single-line, the 4 GHz driving RF signal at optical frequency comb generator is off. We can observe that the receiver sensitivity at the FEC limit (BER of 2×10^{-3}) is achieved at -2.5 dBm and -0.5 dBm for air transmission of 0.65 m and 1.35 m, respectively. The signal to noise ratio decreases as air distance

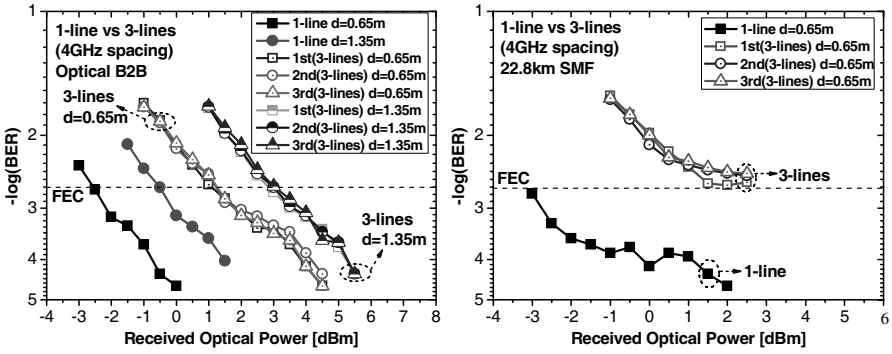

Figure 5. Measured BER performance of 8.9 Gbit/s (single-line) and 26.7 Gbit/s (3-lines with 4 GHz spacing) 16QAM-OFDM W-band wireless transmission without (a) and with (b) 22.8 km SMF fiber transmission.

increases, resulting in higher required optical power at the FEC limit. For 3-lines with 4 GHz spacing, we can see that the receiver sensitivity of the 1st line to reach the FEC limit is 1 dBm and 2.8 dBm for air transmission of 0.65 m and 1.35 m, respectively. There is negligible power penalty among different lines, and about 3.5 dB power penalty between single line case and 3-lines cases at the same air distance. This power penalty is expected, since the optical signal to noise ratio (OSNR) of 3-lines is about 5 dB lower than that of single-line at a given optical power, as indicated in Fig. 3(a).

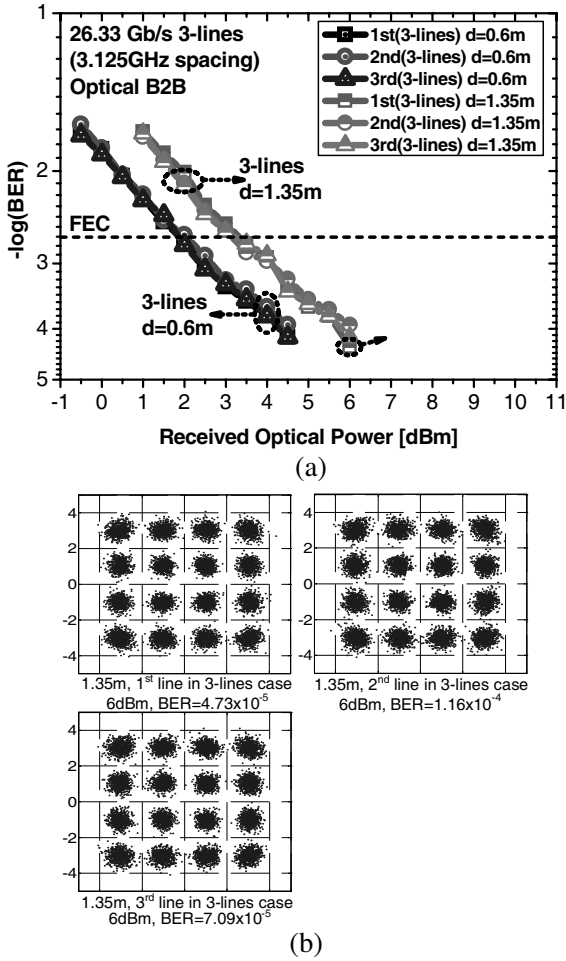

Figure 6. Measured BER performance of 26.33 Gbit/s 16QAM-OFDM signal (3-lines with 3.125 GHz spacing) wireless transmission in optical B2B (a) and received constellations (b).

Figure 5(b) presents the BER performance of 8.9 Gbit/s (single-line) and 26.7 Gbit/s (3-lines with 4 GHz spacing) 16QAM-OFDM W-band signal after hybrid 22.8 km SMF and 0.65 m air transmission. Compared to the optical B2B case, the system performance is degraded when the received optical power into the PD is higher than 0 dBm for single-line case and 2 dBm for 3-lines case. This can be explained that OFDM signal is sensitive to the nonlinearity of the fiber and wireless channel due to its high peak-to-average-power-ratio (PAPR).

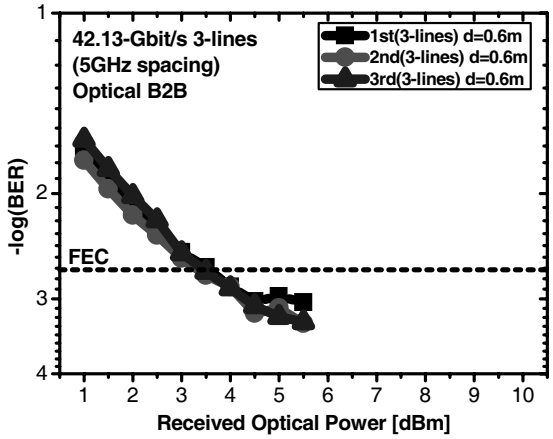

(a)

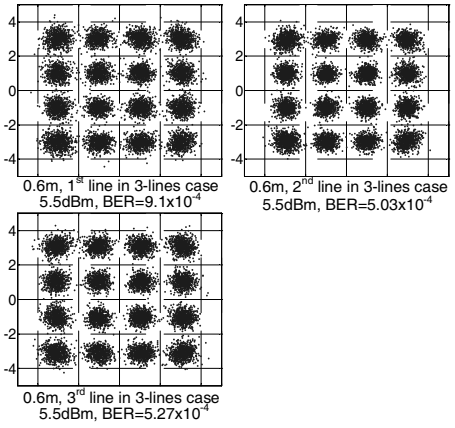

(b)

Figure 7. Measured BER performance of 42.13 Gbit/s 16QAM-OFDM signal (3-lines with 5 GHz spacing) wireless transmission in optical B2B (a) and received constellations (b).

Figure 6(a) and Fig. 7(a) depict the BER curves of 26.33 Gbit/s (3-lines with 3.125 GHz spacing) and 42.13 Gbit/s (3-lines with 5 GHz spacing) W-band signal wireless transmissions. For 3-lines with 3.125 GHz spacing, we can see that the receiver sensitivity of the 1st line to reach the FEC limit is 1.9 dBm and 3.2 dBm for air transmission of 0.6 m and 1.35 m, respectively. 0.9 dB power penalty compared to 3-lines with 4 GHz spacing is attributed to the phase ripple and non-flat frequency response, which degrade the orthogonality of the OFDM subcarriers and introduce inter-symbol interference (ISI). In the case of 3-lines with 5 GHz spacing, we successfully achieve BER performance below the FEC limit for 42.13 Gbit/s 16QAM-OFDM W-band signal after 0.6 m air transmission in the experiment. The receiver sensitivity of the 1st line is 3.5 dBm, and there is negligible power penalty among different comb lines. The received constellations of 26.33 Gbit/s and 42.13 Gbit/s W-band signals are shown in the Fig. 6(b) and Fig. 7(b) as well.

5. CONCLUSION

We have presented a high speed OOFDM photonics-wireless transmission system in 75–110 GHz employing photonic technologies. To our best knowledge, this is the first attempt to combine OFDM modulation and coherent optical frequency division multiplexed techniques to implement a W-band wireless signal up to 42.13 Gbit/s. By developing intra symbol frequency-domain averaging (ISFA) and digital phase-locked loop (DPLL) as an improved channel estimation method, 42.13 Gbit/s 16QAM-OFDM signals at 86 GHz are successfully transmitted over 0.6 m air distance. The proposed system provides for us a promising solution to bring the capacities in optical links to radio links, to realize the seamless integration of high speed wireless and fiber-optic networks.

ACKNOWLEDGMENT

The authors would like to acknowledge the support from Tektronix, Agilent Technologies, Radiometer Physics GmbH, Rohde & Schwarz and u^2t Photonics. This work was partly supported by the National "863" Program of China (No. 2009AA01A347), an EU project EUROFOS, a Danish project OPSCODER and an EU project FP7 ICT-4-249142 FIVER.

REFERENCES

1. Nagatsuma, T., T. Tkakda, H.-J. Song, K. Ajito, N. Kukutsu, and Y. Kado, "Millimeter- and THz-wave photonics towards 100-Gbit/s wireless transmission," *Proc. of IEEE Photonics Society's 23th Annual Meeting*, 385–386, Denver, Colorado, USA, 2010.
2. Ni, W., N. Nakajima, and S. Zhang, "A broadband compact folded monopole antenna for WLAN/WIMAX communication applications," *Journal of Electromagnetic Waves and Applications*, Vol. 24, No. 7, 921–930, 2010.
3. Soltani, S., M. N. Azarmanesh, E. Valikhanloo, and P. Lotfi, "Design of a simple single-feed dual-orthogonal-linearly-polarized slot antenna for concurrent 3.5 GHz WIMAX and 5 GHz WLAN access point," *Jouranl of Electromagnetic Waves and Applications*, Vol. 24, No. 13, 1741–1750, 2010.
4. Ren, X.-S., Y.-Z. Yin, W. Hu, and Y.-Q. Wei, "Compact tri-band rectangular ring patch antenna with asymmetrical strips for WLAN/WIMAX applications," *Jouranl of Electromagnetic Waves and Applications*, Vol. 24, No. 13, 1829–1838, 2010.
5. Yang, B., X.-F. Jin, X.-M. Zhang, H. Chi, and S. L. Zheng, "Photonic generation of 60 GHz millimeter-wave by frequency quadrupling based on a mode-locking SOA fiber ring laser with a low modulation depth MZM," *Jouranl of Electromagnetic Waves and Applications*, Vol. 24, No. 13, 1773–1782, 2010.
6. Navarro-Cia, M., V. T. Landivar, M. Beruete, and M. S. Ayza, "A slow light fishnet-like absorber in the millimeter-wave range," *Progress In Electromagnetics Research*, Vol. 118, 287–301, 2011.
7. Wells, J., "Faster than fiber: The future of multi-Gb/s wireless," *IEEE Microw. Mag.*, Vol. 10, No. 3, 104–112, 2009.
8. Thakur, J. P., W.-G. Kim, and Y.-H. Kim, "Large aperture low aberration aspheric dielectric lens antenna for W-band quasioptics," *Progress In Electromagnetics Research*, Vol. 103, 57–65, 2010.
9. Nee, V. R. and R. Prasad, *OFDM Wireless Multimedia Communications*, Artech House, Boston, 2000.
10. Prasad, R., *OFDM for Wireless Communications Systems*, Artech House, Boston, 2004.
11. Weiss, M., A. Stohr, F. Lecoche, and B. Charbonnier, "27 Gbit/s photonic wireless 60 GHz transmission system using 16-QAM OFDM," *Proc. of International Topical Meeting on Microwave Photonics*, 1–3, Valencia, Spain, 2009.

12. Lin, C.-T, E.-Z. Wong, W.-J. Jiang, P.-T. Shin, J. Chen, and S. Chi, "28-Gb/s 16-QAM OFDM radio-over-fiber system within 7-GHz license-free band at 60 GHz employing all-optical up-conversion," *Proc. of Conference on Lasers and Electro-optics and Conference on Quantum Electronics and Laser Science CLEO/QELS*, 1–2, Baltimore, MD, USA, 2009.
13. Kanno, A., K. Inagaki, I. Morohashi, T. Sakamoto, T. Kuri, I. Hosako, T. Kawanishi, Y. Yoshida, and K.-I. Kitayama, "20-Gb/s QPSK W-band (75–110 GHz) wireless link in free space using radio-over-fiber technique," *IEICE Electron. Express*, Vol. 8, No. 8, 612–617, 2011.
14. Kanno, A., K. Inagaki, I. Morohashi, T. Sakamoto, T. Kuri, I. Hosako, T. Kawanishi, Y. Yoshida, and K.-I. Kitayama, "40 Gb/s W-band (75–110 GHz) 16-QAM radio-over-fiber signal generation and its wireless transmission," *Opt. Express*, Vol. 19, No. 26, B56–B63, 2011.
15. Zibar, D., R. Sambaraju, A. Caballero, J. Herrera, U. Westergren, A. Walber, J. B. Jensen, J. Marti, and I. T. Monroy, "High-capacity wireless signal generation and demodulation in 75- to 110-GHz band employing all-optical OFDM," *IEEE Photon. Technol. Lett.*, Vol. 23, No. 12, 810–812, 2011.
16. You, Y.-H. and J. B. Kim, "Pilot and data symbol-aided frequency estimation for UWB-OFDM," *Progress In Electromagnetics Research*, Vol. 90, 205–217, 2009.
17. Lee, Y.-D., D.-H. Park and H.-K. Song, "Improved channel estimation and MAI-Robust schemes for wireless OFDMA system," *Progress In Electromagnetics Research*, Vol. 81, 213–223, 2008.
18. Liu, X. and F. Buchali, "Intra-symbol frequency-domain averaging based channel estimation for coherent optical OFDM," *Opt. Express*, Vol. 16, No. 26, 21944–21957, 2008.